

EXPERIMENTAL RESULTS FOR NATURAL CONVECTION HEAT TRANSFER IN A CAVITY WITH FLUSH MOUNTED HEAT SOURCES

Ricardo Alan Verdú Ramos

UNESP – Campus de Ilha Solteira – Departamento de Engenharia Mecânica
Av. Brasil Centro, 56 – Ilha Solteira, SP – 15385-000
ramos@dem.feis.unesp.br

Alessandro Tomio Takaki

UNESP – Campus de Ilha Solteira – Departamento de Engenharia Mecânica
Av. Brasil Centro, 56 – Ilha Solteira, SP – 15385-000
takaki@dem.feis.unesp.br

Giancarlo de Souza Damno

UNESP – Campus de Ilha Solteira – Departamento de Engenharia Mecânica
Av. Brasil Centro, 56 – Ilha Solteira, SP – 15385-000
damno@dem.feis.unesp.br

Abstract. In this work, a experimental study of the natural convection heat transfer in a cavity with discrete heat sources flush mounted in one of the walls, simulating electronic components, is carried out. The inferior and superior walls are insulated and the temperature of the opposite wall to the one with heat sources is maintained constant, lower than the environment temperature. The influence of power dissipated by the sources, the cooling temperature, the aspect ratio and the inclination angle of the cavity with respect to the horizontal plane, on the flow and the heat transfer, have all been evaluated. Cubic cavities were built and experimental tests for measure of the temperature were realized by using thermocouples and a data acquisition system controlled by computer, being obtained the temperature fields inside the cavity, as well as the temperature distribution in the wall where the heat sources are mounted. The results were compared with respect to the maximum temperature in the cavity, that is the parameter of larger interest in the problem. Additionally, flow visualization was realized by using the smoke tracing technique generated by burning incense.

Keywords. Natural convection, thermal cavity, heat sources, temperature measurements.

1. Introduction

Among all the environmental factors, temperature is by far the main responsible for electronic component failures. In fact, the flaw rate increases almost exponentially with the operating temperature (Peterson & Ortega, 1990).

Due to the ever-escalating miniaturization of the components, heat flux by unit of volume has been on the increase followed by the temperature levels and consequently increasing the possibility of failure. Therefore a thermal study becomes highly desirable, moreover in the most critical case in which natural convection seems to be the main mechanism of heat transfer, as in electronic components mounted in a closed cavity.

Among the works on this subject, considering a number of different geometries and contour conditions, some can be mentioned: Keyhani *et al.* (1988), Chadwick *et al.* (1991), Du and Bilgen (1992), Ho and Chang (1994), Hsu *et al.* (1997), Ramos *et al.* (1998), Sezai and Mohamad (2000), to name but a few.

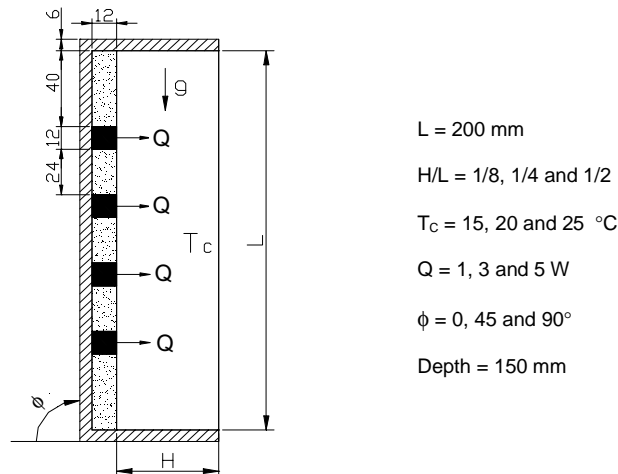


Figure 1. Thermal cavity with flush-mounted heat sources in one of the walls, simulating electronic components.

In the present work, the convective flow in a thermal cavity with discrete heat sources embedded along one of the walls, simulating electronic components, according to Fig. (1), has been experimentally studied.

The temperature field inside the cavity and the temperature distribution along the wall where the heat sources are mounted, as well as the maximum temperature in the cavity (T_{max}), the most interesting parameter in the problem, have been determined, as a function of the dissipated power (Q), opposite wall cooling temperature (T_c), cavity aspect ratio (H/L) and position angle (ϕ). For the basic case (see below), flow visualization by means of a smoke tracing technique is also accomplished.

Three values are selected for each one of the parameters, resulting the cases presented in Tab. (1). In particular, the case 2, in which $Q = 3W$, $H/L = 1/4$, $\phi = 90^\circ$ and $T_c = 20^\circ C$, is assumed to be the basic case for the sake of comparison of results.

Table 1. Description of the cases considered for the parametric analysis of the problem.

Cases	Q (W)	H/L	ϕ	T_c ($^\circ C$)
1	1	1/4	90°	20
2	3	1/4	90°	20
3	5	1/4	90°	20
4	3	1/8	90°	20
5	3	1/2	90°	20
6	3	1/4	45°	20
7	3	1/4	0°	20
8	3	1/4	90°	15
9	3	1/4	90°	25

2. Experimental Procedure

In order to accomplish the experimental tests, a constructive form of the cavities has been designed so as to make it easy to change the geometrical configuration, selectable from $25 \times 200 \times 150$, $50 \times 200 \times 150$ and $100 \times 200 \times 150$ mm. The cavities were constituted by a central piece assembled with three walls of fiberglass (4mm), forming a "U", a front wall of acrylic (12mm), one lateral part (constituting one of the walls of a cold thermal reservoir) and opposite to it another lateral piece contained the embedded discrete heat sources.

The heat sources themselves were comprised of resistances made of *Kanthal* 0.5 mm-diameter wire, electrically insulated, inserted along a longitudinal hole of 6 mm of diameter of an aluminum bar of dimensions $12 \times 12 \times 150$ mm. The heat sources were mounted on a plate of fiberglass, its surface finished with plastic mass and fine sandpaper, and the spaces between the heat sources and between the upper and lower walls were filled with expanded polyurethane. Four DC suppliers (*Dawer PS 3003 D*), covering the range 0-30 Volts and 0-3 Amperes, were deployed in order to obtain the power specified for the experiments.

The thermal reservoirs were made of fiberglass, except for the right internal wall that was made of copper (3mm). The water enters in the reservoirs by the inferior part and leaves by the superior part, maintaining the uniform temperature on the whole copper wall. All external surfaces of the cavity, except for the frontal surface, were thermally insulated from the external environment by means of Styrofoam (25mm).

Figure (2) shows a schematic representation of the constructive details of the thermal cavity.

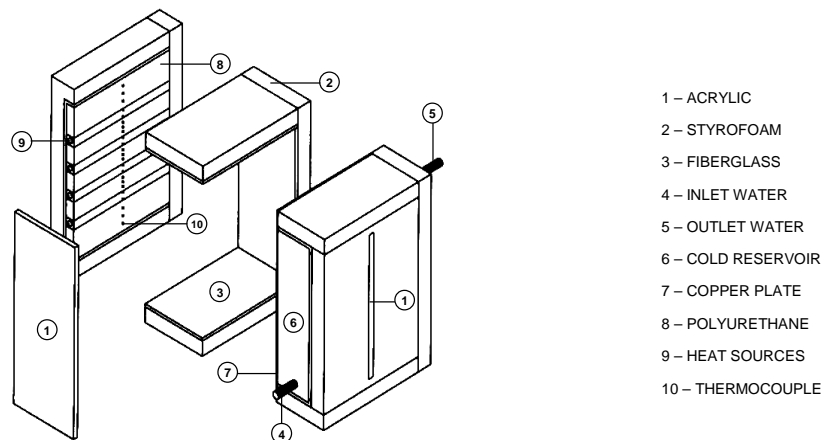


Figure 2. Schematic representation of constructive details of the thermal cavity.

For the temperature measurements, type K (Copper-Constantan) AWG 36 thermocouples, indicated to measure temperatures in the range from 0 to 350°C with precision of $\pm 0,4\%$, were employed. The thermocouples were made through an apparatus specially developed. All the thermocouples were calibrated according to a special bulb thermometer, reaching a precision of 0.05°C. The thermocouples were immersed in a thermostatic water bathing with temperature range from 10 to 95°C and temperatures were evaluated each 5°C, approximately. Three thermocouple readings were determined for each defined temperature, as well as the average and the standard deviation were calculated. Carefully plotted curves for the heating and cooling processes for each one of the thermocouples in the bathing have shown no hysteresis effect and a negligible variation was found among the correlations for each one of the thermocouples, in such a way that a single linear curve could be assumed for all the thermocouples.

Initially, 23 thermocouples were fixed in the wall with the heat sources. Later on, 6 thermocouples more were felt necessary and installed around the last-from-the-top heat source, 4 in the longitudinal direction and 2 in the traverse direction of the wall, to evaluate the conduction heat transfer through the wall, as shown in Fig. (3). In addition, 3 thermocouples were installed along the cold water reservoir wall: one at the center, one at the bottom (close to the water admission) and another at the top (close to the water outlet).

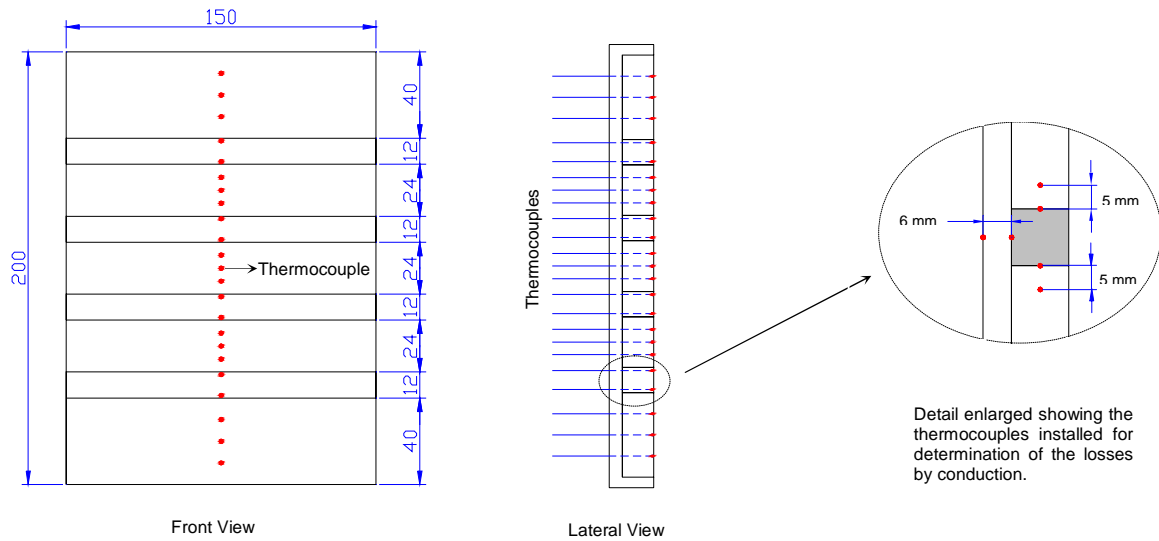


Figure 3. Outline of the positioning of the thermocouples in the wall where the heat sources are mounted.

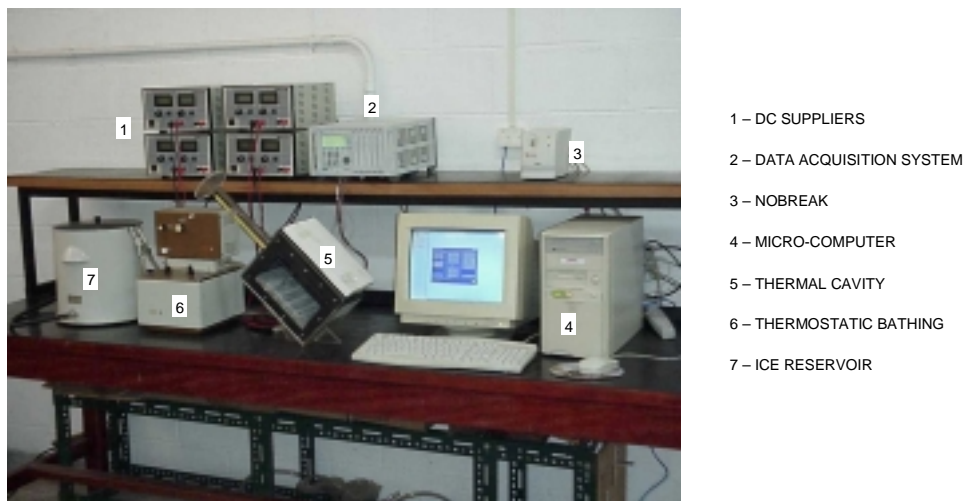
To obtain the temperature field inside the cavities there was a need for the construction of proper probes and respective positioning device, some probes containing 10 thermocouples, for the aspect ratio of 1/2 and 1/4, and others with 5 thermocouples, for the aspect ratio of 1/8. Fig. (4) shows the probes, their thermocouples and positioning system built to move them inside the cavities.



Figure 4. Thermocouple probes and positioning system for temperature measurements inside the cavities.

A data acquisition system (*HBM-MGCPlus*) was employed for the temperature measurements, with a rack in which can be mounted up to 6 amplifiers with 8 channels each, although in the experiments just 4 amplifiers were needed, amounting to 32 channels. From all options available, a parallel interface has been chosen to connect the device to the microcomputer. That data system has an integrated circuit that converts the analogical data of a module simultaneously to digital values in parallel, conditioning the data that will be sent to the computer, allowing for an independent acquisition rate for each channel. Compared to other multiplexed arrangements, capable of reading only one port at a time, this system lends to a continuous reading of the filtered signal for each channel, ruling out interferences, increasing, therefore, reading stability and immunity, indispensable features to its proper application. Also the system executes according to thermocouple type a suitable electronic compensation, making it unnecessary any previous calibration.

After the assembly of the experimental apparatus shown in Fig. (5), the DC suppliers were regulated with the specified dissipation power and the thermostatic bathing was put into operation to maintain constant the temperature of the cold wall. Once reaching steady state, the measurements were initiated, simultaneously acquiring the temperature readings of all the thermocouples of the probe for 60 seconds to a sampling frequency of 1Hz for each measure position (displacement of 5 in 5 mm). Those data were exported to a *Microsoft Excel* spreadsheet, in which the average of the 60 temperature values was calculated (for 60 seconds) for each thermocouple. *Tecplot 8.0* was employed to build the temperature fields with the averaged data; whereas the temperature distributions along the wall with heat sources were plotted using *Excel*.



- 1 – DC SUPPLIERS
- 2 – DATA ACQUISITION SYSTEM
- 3 – NOBREAK
- 4 – MICRO-COMPUTER
- 5 – THERMAL CAVITY
- 6 – THERMOSTATIC BATHING
- 7 – ICE RESERVOIR

Figure 5. Photo of the experimental assembly for temperature measurements in the thermal cavity.

Visualization methods allow for a detailed analysis of a problem without the introduction of flow intrusive probes. There are several references on this subject such as Goldstein (1983), Merzkirch (1987), Yang (1989) and Freymuth (1993), which present many flow visualization applications to solve several kinds of problems. Success in obtaining good results is directly related to the proper choices of technique, lighting, image capture and naturally to the equipment used.

Although the best lighting would have been a high powered laser sheet, an alternative illumination system was constructed with a 1000 W halogen lamp and the light sheet was obtained using a black and white negative slide with a printed transparent slit, produced from high contrast photography of a narrow line left by a laser beam on a white paper sheet. Figure (6) shows a schematic representation of details of this illumination system constructed from a old apparatus for enlarging photos.

Figure (7) shows the experimental setup for the flow visualization inside the thermal cavity. It is quite similar to the one established for the temperature measurements, just by removing the probes and the positioning mechanism while adding the lighting device.

After the assembly of the experimental apparatus, the DC suppliers were regulated with the specified dissipation power and the thermostatic bathing was put into operation to maintain constant the temperature of the cold wall, according to the case 2, described in Tab. (1). Once reaching steady state, two flow visualization techniques were attempted.

The first method employed solid micro particles (dimensions from 50 to 100 μ m) in water, in particular, polypropylene micro particles (*Pliolite*), that have near the same density as water and good reflection properties, that is, when illuminated, they scatter light, allowing for observation of their movement and, consequently, the image capture.

The second method employed injection of smoke in air. In particular, among the several existent choices the smoke generation (tobacco, pitch, oil, etc.), incense was selected, because it is a cheap non-toxic easily manipulated material. Moreover, the smoke particles produced were small enough to follow the flow to be studied, but large enough to diffuse

the light, so that the flow could be registered by photography. The incense smoke has been carefully injected through a small aperture in the cavity top, to avoid flow disturbances.

For image registration, a SLR (*Single Lens Reflex*) 35 mm *Nikon F4s* camera equipped with different accessories and objectives, black & white professionals films *KODAK T-MAX* type 135 with negatives 24×36 mm (ISO 100, 400 and 3200) as well as a digital photographic camera *Sony MVC-CD250*, with resolution of 2.1 Mega pixels, 2X optical and 3X digital zoom modes, were employed and *Corel Photo Paint 10* has been used to post-process the images resulting from the capture phase.

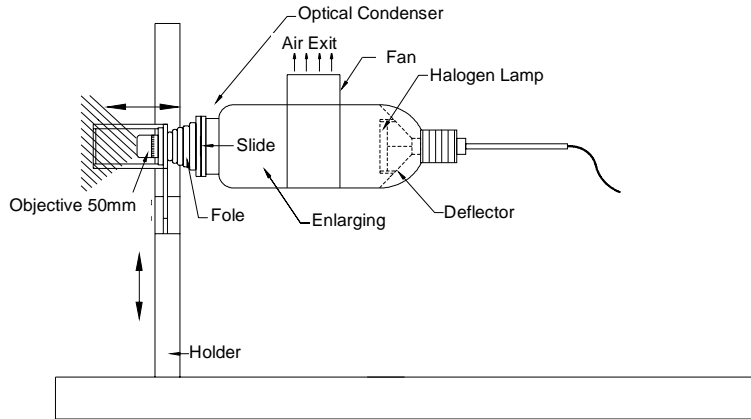


Figure 6. Schematic representation of constructive details of this illumination system.

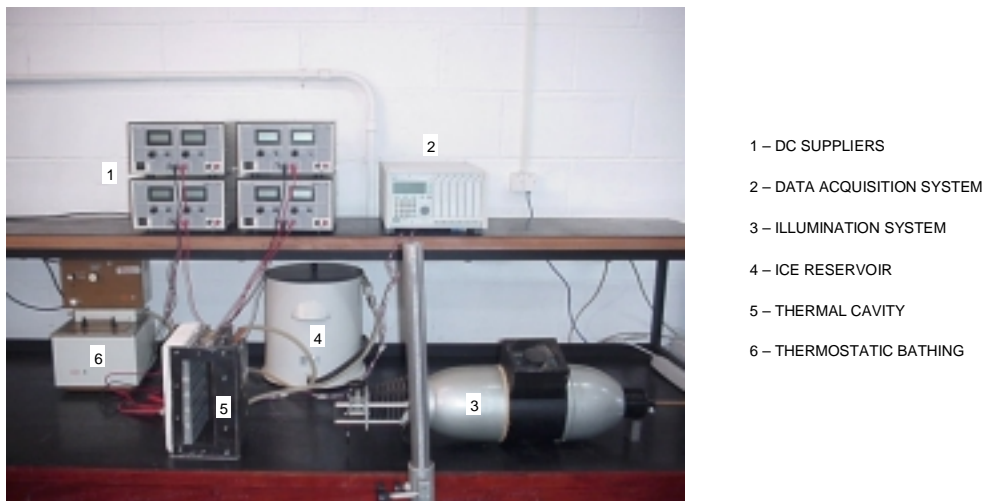


Figure 7. Photo of the experimental assembly for flow visualization in the thermal cavity.

3. Experimental Results

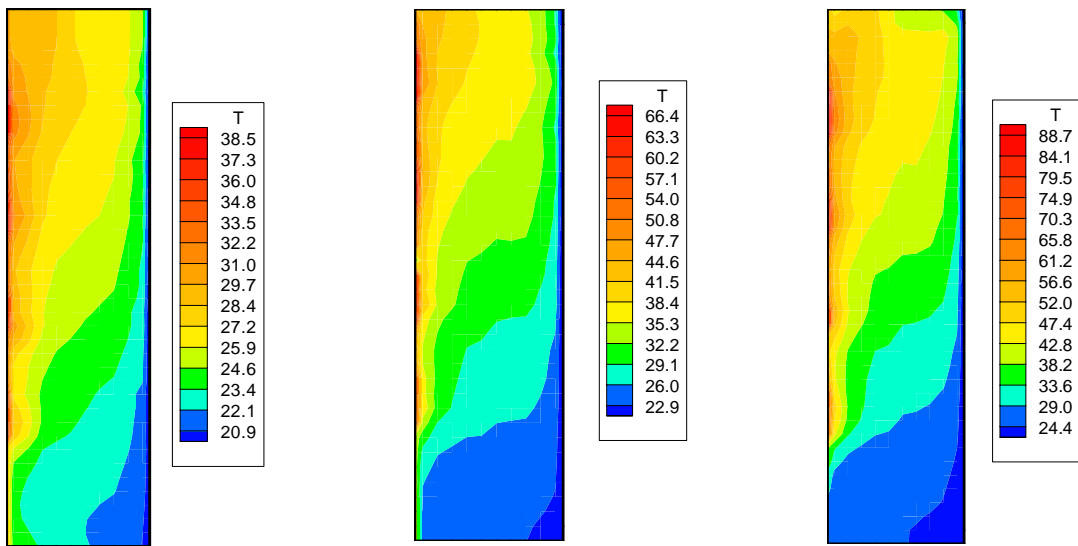
Figure (8) presents the experimental results for the isotherms inside the cavity, for each one of the cases considered in Tab. (1).

Figures (9) to (12) show the temperature profiles in the wall with heat sources, as a function of the power dissipated by the heat source, of the aspect ratio, of the inclination angle and of the cold wall temperature, respectively.

Table (2) shows the maximum temperature values in the cavity, for each one of the cases considered, for comparison effect.

Figure (13) shows a photo of the flow visualization inside the cavity, for the basic case considered (case 2), by using the smoke tracing technique.

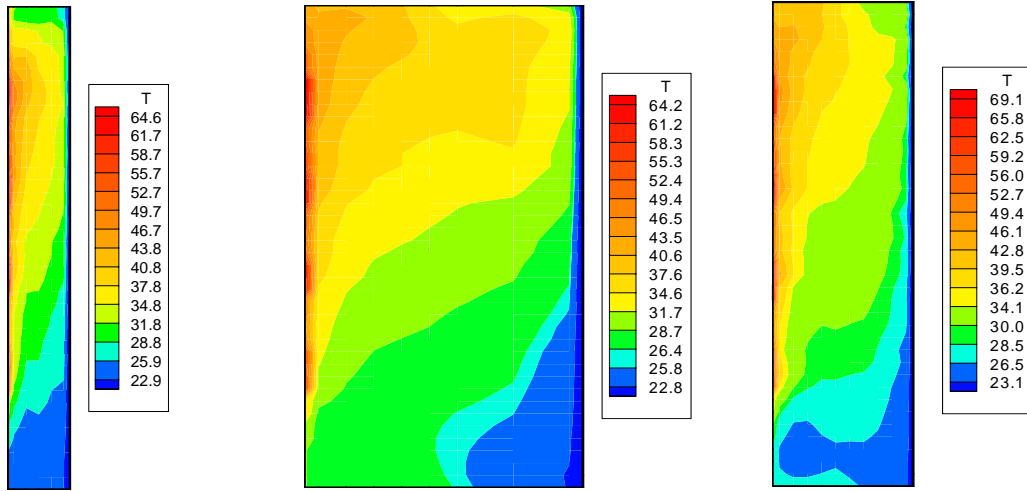
Some conduction heat losses were verified in the experiment and evaluated, in such a way that it has been possible to calculate the actual power supplied for the heating of the air inside the cavity. Table (3) shows the values of the temperature gradient for the polyurethane and fiberglass and the estimate of the heat loss by conduction. In this table, q is the heat flux per unit of area, k is the coefficient of thermal conductivity, ΔT is the difference between two measured temperatures and Δl is the distance between the temperature measurements.



Case 1

Case 2

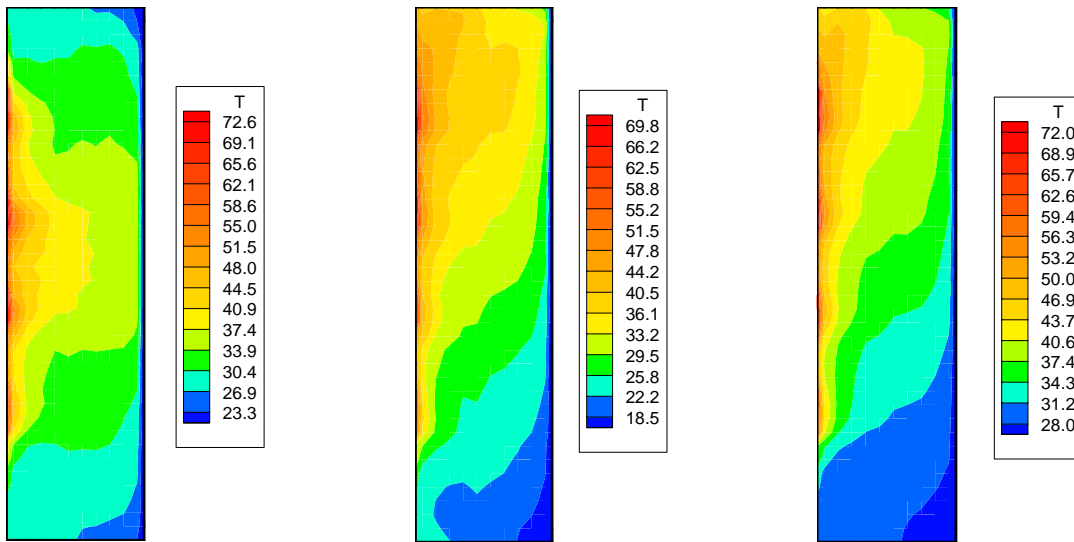
Case 3



Case 4

Case 5

Case 6



Case 7

Case 8

Case 9

Figure 8. Experimental results for isotherms inside the cavity, for each case considered in Table 1.

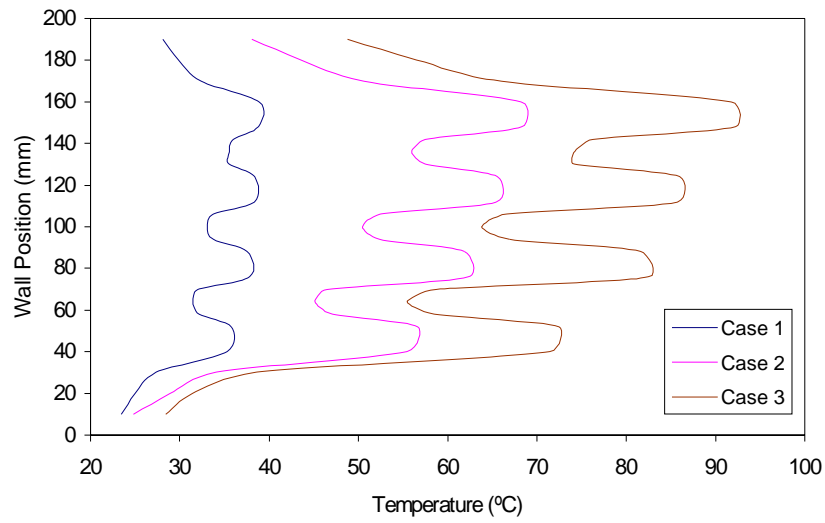


Figure 9. Temperature profiles in the wall with heat sources, as a function of the power dissipated.

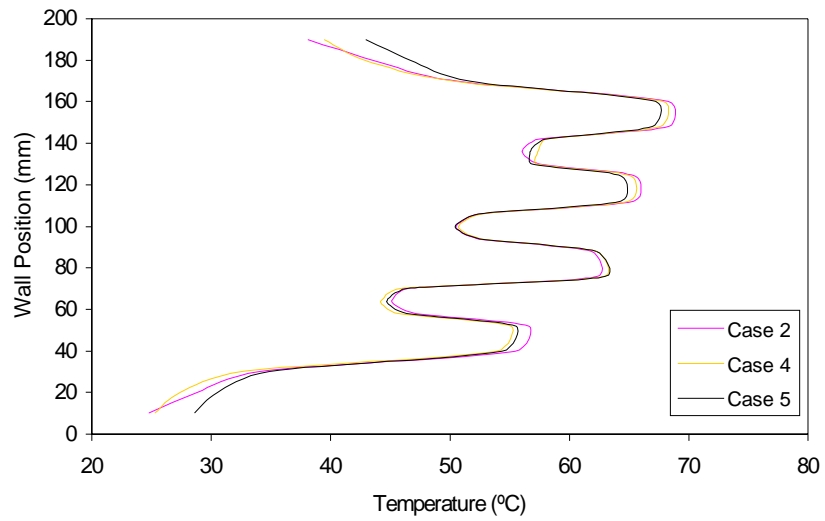


Figure 10. Temperature profiles in the wall with heat sources, as a function of the aspect ratio.

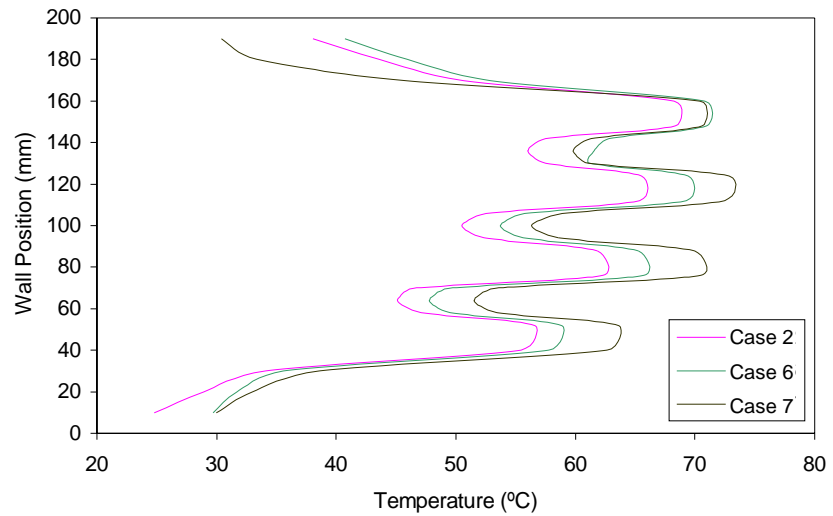


Figure 11. Temperature profiles in the wall with heat sources, as a function of the inclination angle.

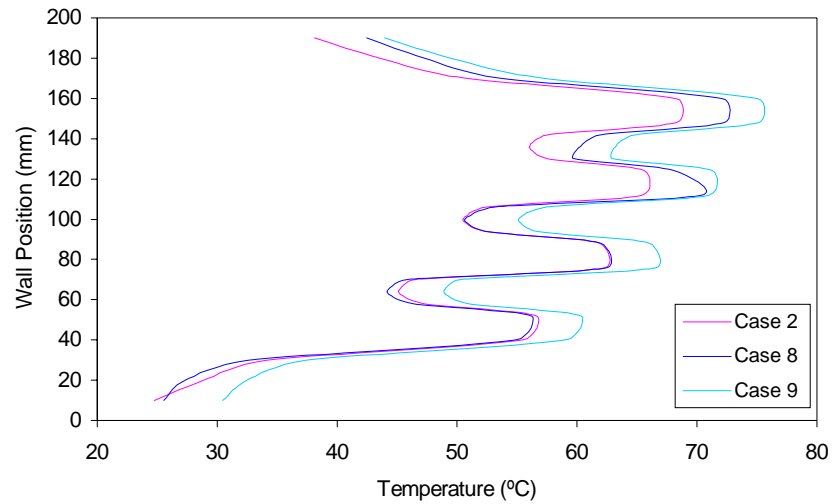


Figure 12. Temperature profiles in the wall with heat sources, as a function of the cold wall temperature.

Table 2. Maximum temperature values, as a function of the case considered.

Cases	Q (W)	H/L	ϕ	T_c (°C)	T_{max} (°C)
1	1	1/4	90°	20	38.9
2	3	1/4	90°	20	68.4
3	5	1/4	90°	20	92.3
4	3	1/8	90°	20	61.7
5	3	1/2	90°	20	61.3
6	3	1/4	45°	20	72.0
7	3	1/4	0°	20	75.1
8	3	1/4	90°	15	72.4
9	3	1/4	90°	25	75.2



Figure 13. Flow visualization with smoke tracing technique, for the basic case considered (case 2).

Table 3. Estimate of the heat conduction losses through the wall with heat sources.

Local	K (W/m°C)	ΔT (°C)	$\Delta\eta = \eta_2 - \eta_1 $ (m)	$q = k\Delta T / \Delta\eta$ (W/m ²)
Polyurethane (superior)	0.32	5.1	0.005	326.4
Polyurethane (inferior)	0.32	10.3	0.005	659.2
Fiberglass (lateral left)	0.035	5.2	0.006	30.3

4. Concluding Remarks

In general, it has been observed that close to the wall with heat sources the isotherms have behaved like a boundary layer, while appearing parallel to the walls with prescribed temperatures and approximately perpendicular to the insulated walls. However, for the horizontally positioned cavity, a distinct configuration have showed up, mostly due to the ascending hotter air coming from the lower central area and the corresponding colder air descending from the top.

With respect to the temperature distribution along the wall with the heat sources, it has been observed that, for every case considered, there has been a sudden temperature increase near and over the heat sources. In addition, each heat source has suffered the effects from the one located just below, in such a way that although the sources dissipate the same power by design, a step distribution in temperature occurred along the wall. In the case of the horizontal cavity, the largest temperature levels could be detected right over the central heat sources, although, contrary to expectations, no perfect symmetry in relationship to the central plane has been detected.

It has been observed that the temperature increased with both, increasing power and diminishing cavity position angle, although for the latter, the effects have been considerably slighter. Changes to the cold wall temperature as well as to the aspect ratio have produced only a minor effect on the temperature levels in the cavity, mainly because the power dissipated by the heat sources were too low to be able to cause some significant increment in the velocity of circulation inside the cavity and therefore causing noticeable alterations in the temperature field.

From the smoke-injection flow visualization inside the cavity, the clockwise circulation of the air coming from the wall with heat sources and traveling towards the cold wall could be observed. Also, cells of smaller circulation paths respectively along the upper and the lower cavity areas, as well as the presence of a stagnation cell in the central area of the cavity, were clearly distinguished.

It has not been possible to accomplish the flow visualization in water, since it would have been necessary larger heat dissipation than the actually employed for the resistances that constitute the heat sources. The right step would have been either to change the resistances, watching carefully that the maximum temperature allowed in the source should not go over about 95°C in order to avoid steam buildup in the proximities of the heat sources, or to use solid micro particles of smaller dimension and lower density, but those changes will be object of future research.

With the *Nikon F4s* SLR 35 mm camera the images captured weren't of a very high quality, mostly due to a poor illumination setup and, consequently, to the impossibility of finding a relationship between the exposition time and the opening of the diaphragm of that camera. The problem has been solved with the help of the *Sony MVC-CD250* digital camera, which allowed the capture of quite good images of the flows employing the same brightness as previously. It is believed that will be possible to obtain even better results with just an improvement of the illumination system.

From the results obtained for the losses of heat, it has been deduced that the perfect isolation was not obtained. Knowing that the total heat dissipated theoretically by the heat sources in the basic case is $Q = 3W$, which corresponds to a volumetric dissipation of the order of $q = 138,888 \text{ W/m}^3$, taking into consideration that the volume of the sources was 0.000216 m^3 ($0.012 \times 0.012 \times 0.15 \text{ m}$), ($0.012 \times 0.15 \text{ m}$) and supposing as perfect the isolation of the superior, inferior and lateral left surfaces and that all generated heat has been transferred to the interior of the cavity from the lateral right surface (the heat sources wall), we would have a heat flux in this surface of the order of $q = 1,667 \text{ W/m}^2$, once the area of the surface is of 0.0018 m^2 . In agreement with the experimental measures, it is verified that the largest part of the generated heat is not going to the interior of the cavity, that is to say, 19.5% are driven towards the polyurethane that is above the heat source, 39.5% are bound to the polyurethane that is around the heat source and 1.8% it is driven towards the fiberglass wall in the lateral left of the heat source, remaining just about 39.2% to the interior of the cavity, those these data measured only for the lowest source, although the almost the same behavior must be expected for the other heat sources as well.

As possible sequences to the present work, improvements in the constructive aspects of the cavity as well as in the experimental assembly, e.g., in terms of thermal insulation and choice of resistances, as well as in the experimental procedures, e.g., illumination system, visualization technique, test of new particles and fluids, have already been planned, aiming towards much better images of the flows in such a way that comparison with numeric results available can therefore be performed.

5. Acknowledgement

The authors wish to acknowledge FAPESP, for the scholarships granting (Processes 01/05794-8 and 01/05795-4), as well as for the financing of the project in which this work is inserted (Process 00/00632-7).

6. References

- Chadwick, M.L., Webb, B.W. and Heaton, H.S., 1991, "Natural Convection from Two-Dimensional Heat Sources in a Rectangular Enclosure", *International Journal of Heat and Mass Transfer*, Vol. 34, No. 7, pp. 1679-1693.
- Du, Z.G. and Bilgen, E., 1992, "Coupling of Wall Conduction with Natural Convection in a Rectangular Enclosure", *International Journal of Heat and Mass Transfer*, Vol. 35, No. 8, pp. 1969-1975.

- Freytmuth, P., 1993, "Flow Visualization in Fluid Mechanics", Review of Sciences and Instruments, Vol. 64, No. 1, pp.1-18.
- Goldstein, R.J., 1983, "Optical Systems for Flow Measurement: Shadowgraph, Schlieren and Interferometric Techniques", in: Fluid Mechanics Measurements, ed. by Goldstein, R.J., pp.377-422, Hemisphere Publishing Co., Washington.
- Ho, C.J. and Chang, J.Y., 1994, "A Study of Natural Convection Heat Transfer in a Vertical Rectangular Enclosure with Two-Dimensional Discrete Heating: Effect of Aspect Ratio", International Journal of Heat and Mass Transfer, Vol. 37, No. 6, pp. 917-925.
- Hsu, T.H., Hsu, P.T. and Tsai, S.Y., 1997, "Natural Convection of Micropolar Fluids in an Enclosure with Heat Sources", International Journal of Heat and Mass Transfer, Vol. 40, No. 17, pp. 4239-4249.
- Keyhani, M., Prasad, V. and Cox, R., 1988, "An Experimental Study of Natural Convection in a Vertical Cavity with Discrete Heat Sources", Journal of Heat Transfer, Vol. 110, pp.616-624.
- Merzkirch, W., 1987, "Flow Visualization", Academic Press Inc., Orlando-FL, USA.
- Peterson, G.P. and Ortega, A., 1990, "Thermal Control of Electronic Equipment and Devices", Advances in Heat Transfer, Vol. 20, pp. 181-314.
- Ramos, R.A.V., Dias Júnior, T. and Milanez, L.F., 1998, "Numerical and Experimental Analysis of Natural Convection in a Cavity with Flush Mounted Heat Sources on a Side Wall", Proceedings of the 6th International Conference on Thermal Phenomena in Electronic Systems, pp. 130-134, Seattle, USA.
- Sezai, I. and Mohamad, A.A., 2000, "Natural Convection from a Discrete Heat Source on the Bottom of a Horizontal Enclosure", International Journal of Heat and Mass Transfer, Vol. 43, pp. 2257-2266.
- Yang, W.-J., 1989, "Handbook of flow visualization", Ed. Taylor & Francis.